Journal of Oceanography
Vol. 48, pp. 221 to 230. 1992

New Detection Method for XBT Depth Error and Relationship Between the Depth Error and Coefficients in the Depth-Time Equation*

KIMIO HANAWA and TAMAKI YASUDA

Department of Geophysics, Tohoku University, Sendai 980, Japan

(Received 9 December 1991; in revised form 24 February 1992; accepted 24 February 1992)

New CTD-XBT (T-7 probe) comparison data are analyzed, which provide additional evidence of XBT depth error and support previous results (Hanawa and Yoritaka, 1987; Hanawa and Yoshikawa, 1991). The depth difference between the corrected and uncorrected data is about 26 m at 750 m. In the present study, new data processing procedures by which the depth errors are automatically detected, are developed and adopted. In the new method, first, temperature gradients (TG) of XBT and CTD profiles are calculated. Then, 20 m segment of the XBT-TG profile which should fit to the CTD-TG profile of 20 m segment to be referred to is searched in the XBT-TG profile. Actually, this is achieved by shifting the XBT-TG profile of 20 m segment so as to minimize the area surrounded by both TG profiles. The shifted depth of XBT-TG profile for CTD-TG profile can be regarded as the XBT depth error. This processing is repeated at intervals of 5 m from 10 m to 790 m of CTD-TG profile. The relationship between the scatter of the quadratic depth-time equation coefficients and the depth error is also discussed. It is shown that when the two coefficients have a certain relationship, the depth differences between the plural depth-time equations are small, even if the two coefficients of those equations have apparently very different values.

1. Introduction

When CTD and XBT measurements are conducted repeatedly along an observational line, the pseudo-undulation of the isotherms ("*XBT wave*") appears in vertical temperature cross section. This is obviously due to depth error in the XBT data and its existence has already been pointed out by several authors (e.g., Flierl and Robinson, 1977; Seaver and Kuleshov, 1982; Heinmiller *et al.*, 1983).

Hanawa and Yoritaka (1987, hereafter HY1) and Hanawa and Yoshikawa (1991, HY2) reported that the actual fall rate of XBT probes made by the Japanese licensed manufacturer, Tsurumi-Seiki Co LTD, is much faster than that estimated by the depth-time equation provided by the XBT manufacturer. A recent report by Singer (1990) reached nearly the same conclusion, using the XBT probes manufactured by Sippican Inc., U.S.A.

An additional CTD-XBT comparison experiment was conducted in the sea south of Japan by the Physical Oceanography Group of Tohoku University. In the first part of this report, we will describe the results of this comparison experiment. Although there is the manual handling stage in the data processing procedures adopted in HY1 and HY2, in the present analysis we adopted

*This paper was presented and discussed in the Ad Hoc Meeting of the IGOSS Task Team on Quality Control for Automated System, held in Marion, Massachusetts, *U.S.A.* in June 3–6, 1991.

newly developed processing procedures, by which the depth error is automatically detected by computer. In the second part, the relationship between the scatter of two coefficients of the quadratic depth-time equations and the depth difference is briefly discussed.

2. The Comparison Experiment and Newly Developed Data Processing Procedures

2.1 CTD-XBT comparison experiment

The CTD-XBT comparison experiment was conducted on the line of Tokyo–Ogasawara Line Experiment (TOLEX) by the R/V *Hakuho Maru* KH-91-1 cruise (OMLET Cruise), belonging to Ocean Research Institute, University of Tokyo, in February 1991 (see Fig. 1). TOLEX is the monitoring program of the Kuroshio current system made by the Physical Oceanography Group, Tohoku University. XBT measurements have been conducted basically bimonthly since August 1988 using a ferry shuttling from Tokyo to the Ogasawara Islands.

The experimental procedures and the apparatus used were the same as reported in HY1 and HY2. Although seven XBT T-7 probes were dropped at seven CTD stations in the comparison experiment, only four profiles were used in the present study since the others were inappropriate for analysis due to wire stretching and noise problems. In this report, we will refer to these data as dataset E. Note that dataset E in HY2 was the data from T-6 probes.

Figure 2(a) shows the CTD temperature profiles and Fig. 2(b) does the temperature difference between CTD data and XBT data calculated by the depth-time equation originally

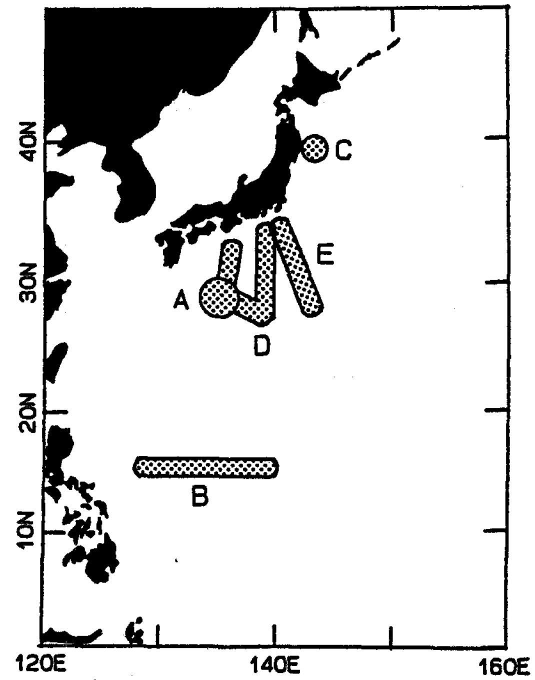

Fig. 1. Locations where CTD-XBT comparison experiments were conducted. New CTD-XBT comparison experiment presented in this study was made in the area denoted by E. Datasets A through D were already reported in HY2.

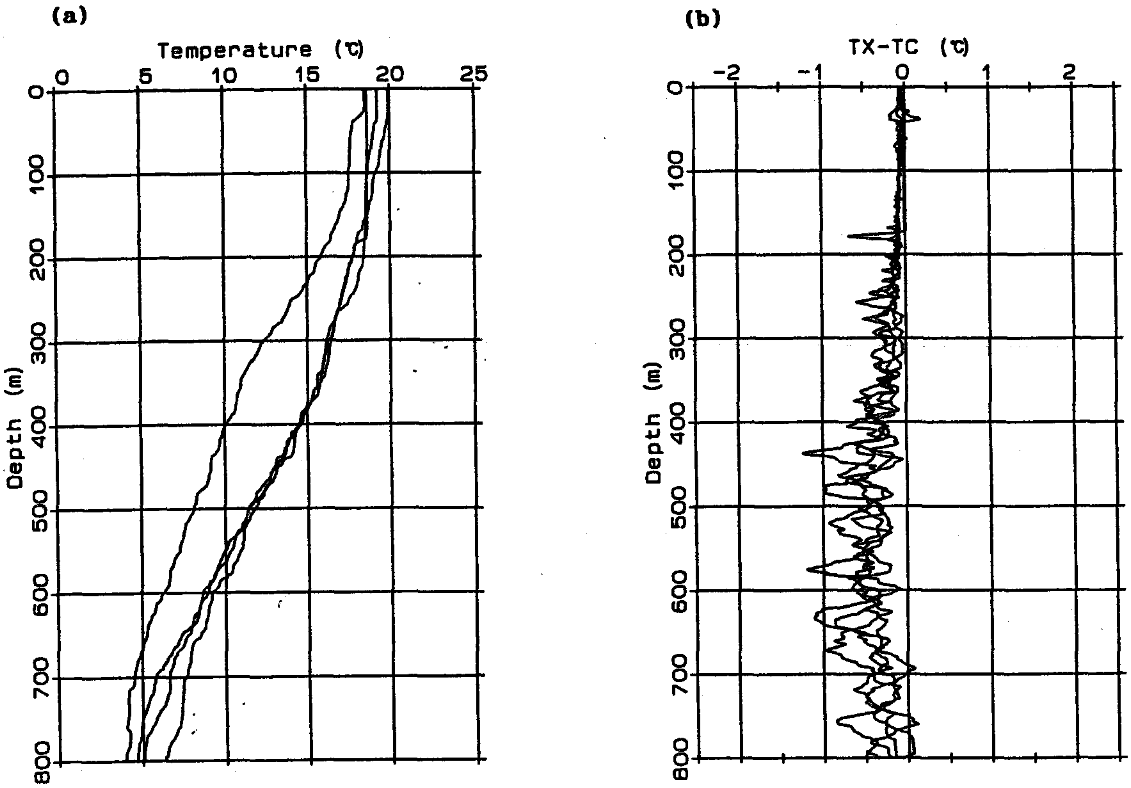

Fig. 2. (a) CTD temperature profiles of the present comparison data (dataset E) and (b) temperature differences of XBT and CTD data. XBT depths were calculated by the equation provided by the XBT manufacturer.

provided by the XBT manufacturer (Eq. (2) of HY2).

2.2 Data processing procedures adopted

To avoid manual handling in the detection of depth error used in HY1 and HY2, new data processing procedures were developed and adopted. The actual procedures are as follows.

(1) Preparation of 1 m-interval data

From the observed raw data, 1 m-interval temperature data are calculated using a linear interpolation scheme for both CTD and XBT data. CTD pressure data are converted to depth data by using the approximate relation equation (Eq. (1) of HY2). The XBT depths are calculated from the depth-time equation provided by the XBT manufacturer (Eq. (2) of HY2).

(2) Filtering

A simple running average with a box-car filter of 11 points (spacing 10 m of CTD data) is applied to both sets of 1 m-interval data.

(3) Calculation of temperature gradient

Temperature gradients (hereafter TG) are calculated from both filtered CTD and XBT data.

(4) Detection of depth difference

20 m segment of the XBT temperature gradient (XBT-TG) profile which should fit to the

CTD-TG profile of 20 m segment to be referred, is searched in the XBT-TG profile. Actually, this is achieved by gradually shifting the XBT-TG profile of 20 m segment so as to minimize the area surrounded by both CTD-TG and XBT-TG profiles. See Fig. 3, which is the explanatory picture of the present method.

The shifting range of XBT-TG is from 50 m above the central depth of CTD-TG profile to be referred to 30 m below that. That is, 81 data of the area are calculated. The shifted depth which gives the minimum value of area can be regarded as the depth error of XBT depth.

In the present analysis, estimations of XBT depth error are made at intervals of 5 m from 10 m to 790 m of the CTD (true) depths. So we can obtain 157 depth difference data for one profile.

(5) Calculation of true elapsed time for XBT

The elapsed times at the depths of true XBT depths are calculated by using the depth-time equation used in estimation of depths of XBT data.

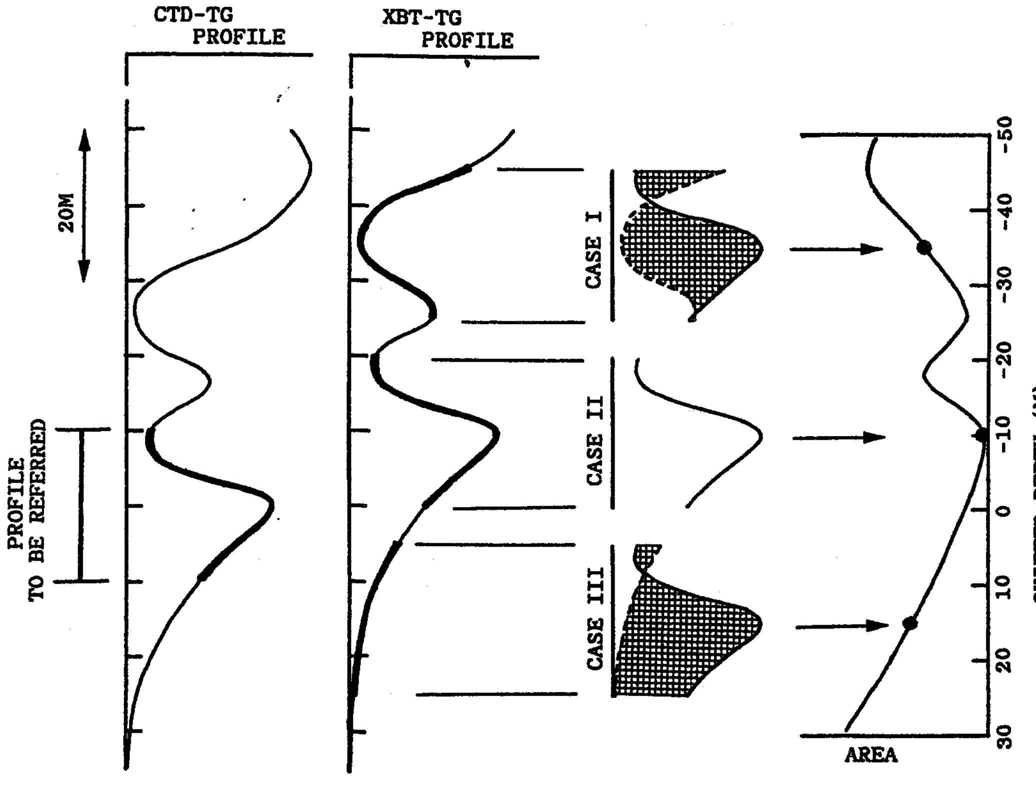

Fig. 3. Explanatory picture of the detection method adopted by the present analysis. First, 20 m segment of CTD-TG (temperature gradient) profile to be referred is set, which is denoted by the thick line in this figure. Then, 20 m segment of XBT-TG profile is also selected and the area surrounded by the two TG profiles is calculated. The shifting depth range of XBT-TG profile is from 50 m above the central depth of CTD-TG profile to be referred to 30 m below that, and therefore 81 data of area are calculated. In this figure, only three cases are shown as examples. Since the area has the minimum value in Case II, the shifted depth of −10 m for XBT-TG profile is regarded as the depth error of XBT data. Same processing is made at intervals of 5 m from 5 m to 790 m of CTD depths.

(6) Estimation of the tentative depth-time equation

Using the dataset of true depths versus the elapsed times of all profiles, a *tentative* depth-time equation is estimated by the method of least squares.

(7) Calculation of new XBT depths by a tentative equation

From the *tentative* depth-time equation, new XBT depths are re-calculated and 1 m-interval XBT temperature data are computed from the observed raw data.

(8) Iteration

Stages 2 through 5 are repeated.

(9) Estimation of final equation

After the above processing is completed, a new (final) equation is estimated using the dataset of true depths versus the elapsed times of all profiles.

3. Results and Comparison with the Previous Results

Figure 4 shows the scatter plot of the true depths of XBT probes as a function elapsed time. Although there are a few data far from the plausible relation, it shows reasonable dependence on some depth-time relation. The reason of existence of the data far from the plausible relation is that due to some *unfavorable* temperature profile, this method could not successfully detect the XBT depth errors at some depth.

Unfavorable temperature profile for the present method means, for example, the vertically constant temperature and/or linearly decreasing temperature within the mixed layer or some

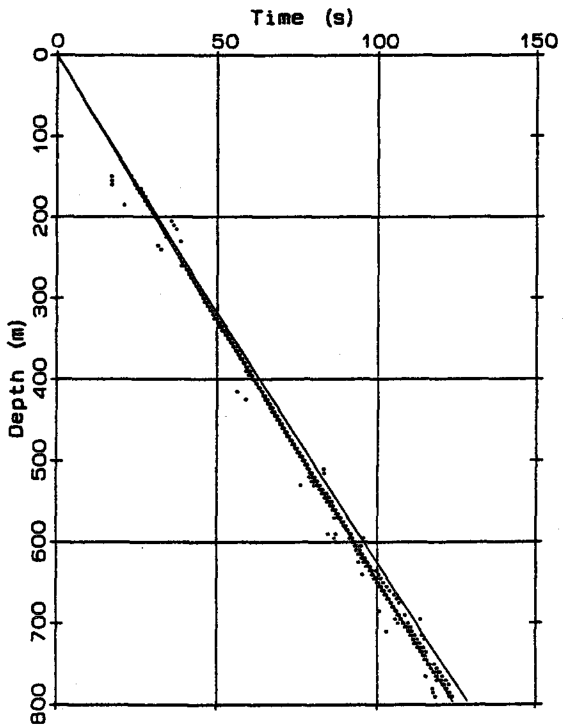

Fig. 4. Scatter plot of the true depths of XBT probes as a function elapsed time. The data of true depth (CTD depth) and elapsed time are obtained at 5 m intervals in CTD depth.

layer. For this situation, the present method tends to fail to detect the depth error, because all the calculated areas are close to zero. Of course, when some noises are contaminated in the XBT or CTD temperature data, same things will happen.

Since the data relatively far from the plausible relation are a few, we estimated the equation from all depth-elapsed time data by the least-squares method. The newly estimated depth-time equation for dataset E is,

$$Z_x = 6.655t - 1.844 \times 10^{-3} t^2. \qquad (1)$$

This equation gives the maximum depth error of 26 m at 750 m compared with the depths calculated by the XBT manufacturer's equation (Eq. (2) of HY2).

Figure 5(a) shows the temperature difference profiles between CTD and XBT data, whose depths are calculated by Eq. (1). Compared with Fig. 2(b), it clearly shows that this new equation can give a good estimation of XBT depths obtained in the present experiment.

Figure 5(b) is same as in (a) but for XBT depths which are calculated by the unified equation proposed in HY2 (Eq. (3) of HY2),

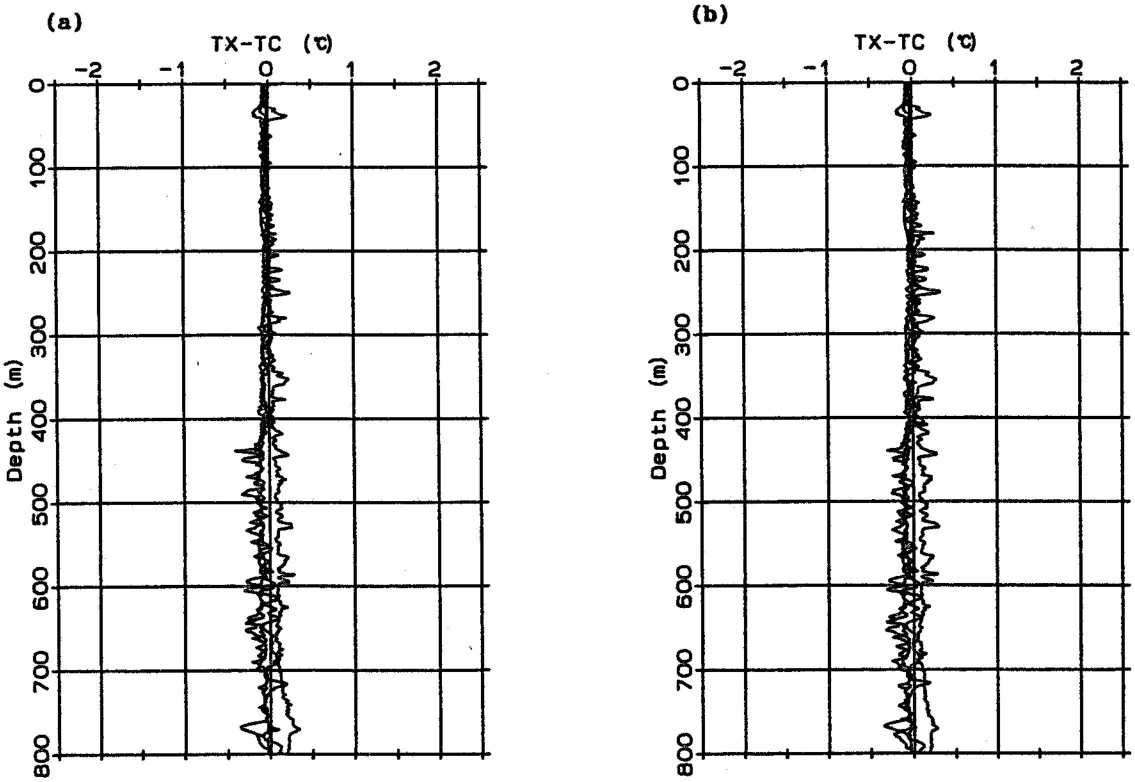

Fig. 5. (a) As in Fig. 2(b) but for using the XBT depths estimated by Eq. (1). (b) As in (a) but for those estimated by Eq. (3) in HY2. Equation (3) in HY2 is an unified equation estimated using the whole data treated in HY2.

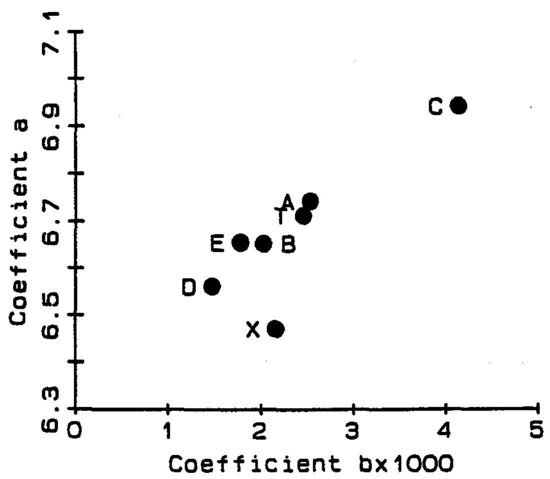

Fig. 6. Relationship between coefficients a and b of depth-time equation for T-7 probe (re-drawn from Fig. 9 of HY2). T means an unified equation for datasets A through D (Eq. (3) in HY2) and X denotes that provided by XBT manufacturer.

$$Z_x = 6.711t - 2.454 \times 10^{-3} t^2. \tag{2}$$

At glance, it seems that Eq. (1) is very different from Eq. (2). However, both temperature difference profiles shown in Figs. 5(a) and (b) are almost same. Actually, the maximum depth difference between the depths given by Eqs. (1) and (2) is within only 2 m in the whole depth range. This reason is the main point to be discussed in the next section.

Figure 6 shows the relationship between the two coefficients a and b, re-drawn from Fig. 9 of HY2: coefficients a and b (defined by positive value) are those multiplied by t and t^2, respectively, in the depth-time equations. The two coefficients of the present Eq. (1) lie near dataset B. That is, the present result strongly supports the authors' previous conclusion in HY1 and HY2: the fall rate of XBT probes is much greater than the velocity given by the XBT manufacturer.

4. Distribution of Depth Differences on Coefficients *a-b* Plane

In this section we will show that, when two coefficients, a and b, in the depth-time equation which is estimated for some dataset, have a special relationship for values of the reference equation or those of other datasets, depth differences estimated by the two equations are not so large.

Figure 7(b) shows profiles of the depth difference between the depth calculated by the reference equation and the other equations with four combinations of coefficients a and b, which are specified on the a-b plane of Fig. 7(a), Cases I through IV. Coefficients a and b of the reference equation were selected as 6.711 and 2.454×10^{-3} respectively, which correspond to Eq. (2) in the present paper (Eq. (3) in HY2, i.e., a unified equation for datasets A through D). Coefficients a and b of Case I (II) were selected as though both a and b are smaller (greater) than those of the reference equation. On the other hand, coefficients of Case III (IV) were set as though when a is greater (smaller) than the reference equation, b is smaller (greater).

In Case I (II), the depth difference is negative (positive) from the surface to about 600 m, it

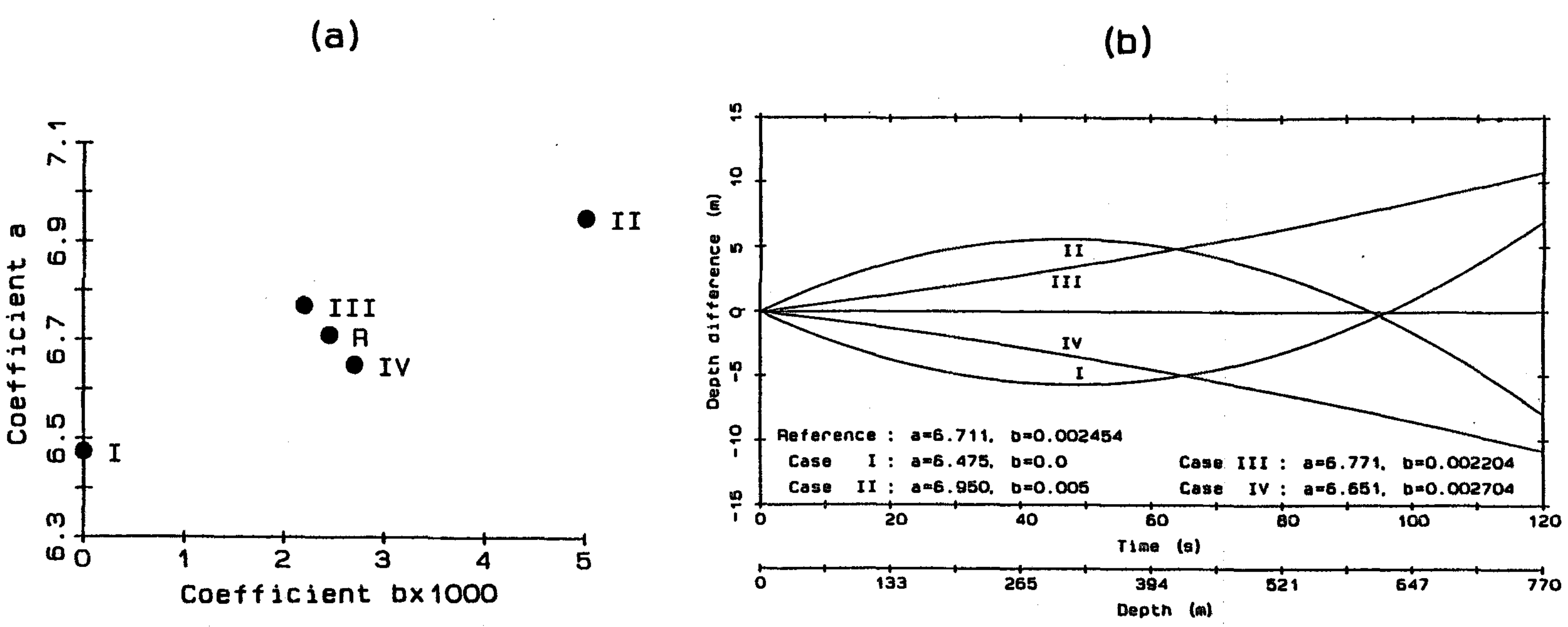

Fig. 7. (a) Combinations of *a* and *b* selected to show examples of depth differences: the reference equation and Cases I through IV. Symbol R denotes the reference equation which is same as T in Fig. 6. (b) Profiles of depth difference for each case from the depths estimated by the reference equation. The depth of abscissa is calculated by the reference equation.

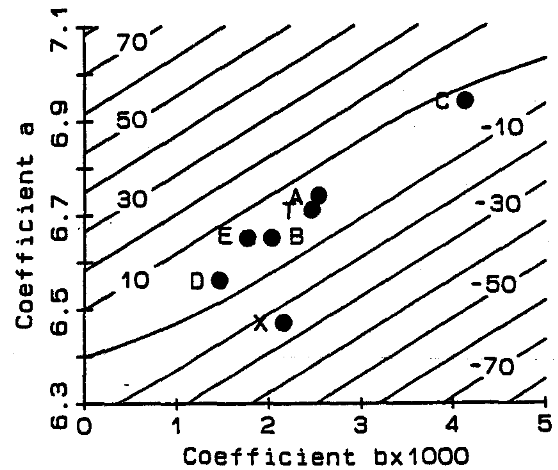

Fig. 8. Distribution of the maximum values of depth difference on coefficients *a*-*b* plane from the reference equation as in Fig. 7. Units in meter.

then crosses zero line and changes to the positive (negative) side. Although coefficients *a* and *b* of Cases I and II are apparently very different from the reference values, the actual depth difference is within plus/minus 10 m from the surface to the reference depth of 770 m. On the other hand, in Case III (IV), the depth difference gradually increases in a positive (negative) direction from surface, and at the reference depth of 770 m it is greater than 10 m. Although coefficients *a* and *b* of Cases III and IV are very similar to the reference values compared with Cases I and II, they do not mean directly that the depth difference is small. That is, the combination of coefficients *a* and *b* is essential to know how the depth difference behaves.

Figure 8 shows the distribution of the maximum values of depth differences between the depths calculated by the reference equation and those by the other combinations of coefficients *a* and *b*. This figure shows that when coefficients *a* and *b* have some special relationship, the depth difference is not so large. This special relationship between coefficients *a* and *b* can be roughly represented as,

$$a = 6.475 + 0.1 \times (b \times 1000). \tag{3}$$

Note that this relation equation, of course, depends on *a* and *b* from the reference equation. The existence of the situation mentioned above simply reflects the character of the quadratic depth-time equation.

Since all coefficients of equations estimated in HY2 and the present study almost satisfy the above relationship, this strongly suggests that we can make a unified depth-time equation.

5. Concluding Remarks

In the present study, the data of new XBT-CTD comparison experiment were analyzed by using the newly developed analytical procedures. The result strongly supported the authors' previous results. That is, actual fall rate of XBT probes is much greater than that given by the XBT manufacturer. Values of coefficients in the equations estimated for individual datasets are different each other. However, as discussed in Section 4, actual depth differences calculated by those equations are not so large, because coefficients have some special relationship. This fact is very fortunate for XBT users, since this means that users are able to make a single unified equation like Eq. (3) in HY2.

Why do coefficients a and b distribute along the specific region as shown in Fig. 7? HY2 speculated that it reflects the scatters of the wire weight and the enamel coating on it. Although the authors believe that this is a basic cause, it seems that Fig. 8 suggests the existence of additional causes, because the scatterness is too large. However, the authors can not specify it yet.

Finally, the authors like to repeat the statement in HY2 on the use of the newly estimated equations. Although an individual investigator can freely use the newly estimated equations for his studies, XBT data sent to the national or international XBT data centers should be those calculated by the equation provided by the XBT manufacturer. That is, the existence of mixed data in the database must be absolutely avoided.

Acknowledgements

The authors would like to express their sincere thanks to the captain, officers and crew and all scientists of the R/V *Hakuho Maru* KH-91-1 cruise (OMLET Cruise) for their cooperation of CTD-XBT comparison experiment. They also thank Y. Yoshikawa and H. Kinoshita for comments in developing the computer software. Discussions in the meeting of the IGOSS Task Team on Quality Control for Automated System held in June 1991 were very useful. The authors also acknowledge comments by an anonymous reviewer.

This study was made as part of OMLET (chairman: Prof. Y. Toba), and as part of the Scientific Research on Priority Areas, "Ocean Fluxes—Their Role in the Geosphere and the Biosphere", which are financially supported by the Ministry of Education, Science and Culture.

References

Fliert, G. and A. R. Robinson (1977): XBT measurements of the thermal gradient in the MODE eddy. *J. Phys. Oceanogr.*, **7**, 300–302.

Hanawa, K. and H. Yoritaka (1987): Detection of systematic errors in XBT data and their correction. *J. Oceanogr. Soc. Japan*, **32**, 68–76.

Hanawa, K. and Y. Yoshikawa (1991): Re-examination of depth error in XBT data. *J. Atmos. Oceanic Technol.*, **8**, 422–429.

Heinmiller, R. H., C. C. Ebbesmeyer, B. A. Taft, D. B. Olson and O. P. Nikitin (1983): Systematic errors in expendable bathythermograph (XBT) profiles. *Deep-Sea Res.*, **30**, 1185–1196.

Seaver, G. A. and A. Kuleshov (1982): Experimental and analytic error of the expendable bathythermograph. *J. Phys. Oceanogr.*, **12**, 592–600.

Singer, J. J. (1990): On the error observed in electronically digitized T-7 XBT data. *J. Atmos. Oceanic Technol.*, **7**, 603–611.